INAF
ISTITUTO NAZIONALE
DI ASTROFISICA
NATIONAL INSTITUTE
FOR ASTROPHYSICS

Publication Year	2021
Acceptance in OA	2022-03-16T16:56:40Z
Title	The SPHERE infrared survey for exoplanets (SHINE). I. Sample definition and target characterization
Authors	DESIDERA, Silvano, Chauvin, G., Bonavita, M., MESSINA, Sergio, LeCoroller, H., SCHMIDT, TOBIAS MARIUS, GRATTON, Raffaele, Lazzoni, C., Meyer, M., Schlieder, J., Cheetham, A., Hagelberg, J., Bonnefoy, M., Feldt, M., Lagrange, A. -M., Langlois, M., Vigan, A., Tan, T. G., Hambsch, F. -J., Millward, M., ALCALA', JUAN MANUEL, BENATTI, SERENA, Brandner, W., Carson, J., COVINO, Elvira, Delorme, P., D'ORAZI, VALENTINA, Janson, M., RIGLIACO, ELISABETTA, Beuzit, J. -L., Biller, B., Boccaletti, A., Dominik, C., Cantalloube, F., Fontanive, C., Galicher, R., Henning, Th., Lagadec, E., LIGI, ROXANNE, Maire, A. -L., Menard, F., MESA, DINO, Müller, A., Samland, M., Schmid, H. M., Sissa, E., TURATTO, Massimo, Udry, S., Zurlo, A., Asensio-Torres, R., Kopytova, T., Rickman, E., Abe, L., Antichi, J., BARUFFOLO, Andrea, Baudoz, P., Baudrand, J., Blanchard, P., Bazzon, A., Buey, T., Carbillet, M., Carle, M., Charton, J., CASCONE, Enrico, CLAUDI, Riccardo, Costille, A., Deboulbé, A., DE CAPRIO, VINCENZO, Dohlen, K., FANTINEL, Daniela, Feautrier, P., Fusco, T., Gigan, P., GIRO, Enrico, Gisler, D., Gluck, L., Hubin, N., Hugot, E., Jaquet, M., Kasper, M., Madec, F., Magnard, Y., Martinez, P., Maurel, D., Le Mignant, D., Möller-Nilsson, O., Llored, M., Moulin, T., Origné, A., Pavlov, A., Perret, D., Petit, C., Pragt, J., Puget, P., Rabou, P., Ramos, J., Rigal, F., Rochat, S., Roelfsema, R., Rousset, G., Roux, A., SALASNICH, Bernardo, Sauvage, J. -F., Sevin, A., Soenke, C., Stadler, E., Suarez, M., Weber, L., Wildi, F.
Publisher's version (DOI)	10.1051/0004-6361/202038806
Handle	http://hdl.handle.net/20.500.12386/31639
Journal	ASTRONOMY & ASTROPHYSICS
Volume	651

A&A 651, A70 (2021)
https://doi.org/10.1051/0004-6361/202038806
© ESO 2021

Astronomy & Astrophysics

The SPHERE infrared survey for exoplanets (SHINE)

I. Sample definition and target characterization*

S. Desidera[1], G. Chauvin[2], M. Bonavita[3,4,1], S. Messina[5], H. LeCoroller[6], T. Schmidt[7,8], R. Gratton[1], C. Lazzoni[1,9], M. Meyer[10,11], J. Schlieder[12,13], A. Cheetham[14,13], J. Hagelberg[14], M. Bonnefoy[2], M. Feldt[13], A.-M. Lagrange[2], M. Langlois[6,15], A. Vigan[6], T. G. Tan[16], F.-J. Hambsch[17], M. Millward[18], J. Alcalá[19], S. Benatti[20], W. Brandner[13], J. Carson[21,13], E. Covino[19], P. Delorme[2], V. D'Orazi[1], M. Janson[13,22], E. Rigliaco[1], J.-L. Beuzit[6], B. Biller[3,4,13], A. Boccaletti[8], C. Dominik[23], F. Cantalloube[13], C. Fontanive[24,1], R. Galicher[8], Th. Henning[13], E. Lagadec[25], R. Ligi[26], A.-L. Maire[27,13], F. Menard[2], D. Mesa[1], A. Müller[13], M. Samland[13], H. M. Schmid[11], E. Sissa[1], M. Turatto[1], S. Udry[14], A. Zurlo[28,29,6], R. Asensio-Torres[13], T. Kopytova[13,30,31], E. Rickman[14], L. Abe[25], J. Antichi[32], A. Baruffolo[1], P. Baudoz[8], J. Baudrand[8], P. Blanchard[6], A. Bazzon[11], T. Buey[8], M. Carbillet[25], M. Carle[6], J. Charton[2], E. Cascone[1], R. Claudi[1], A. Costille[6], A. Deboulbé[2], V. De Caprio[19], K. Dohlen[6], D. Fantinel[1], P. Feautrier[2], T. Fusco[33], P. Gigan[8], E. Giro[1,26], D. Gisler[11], L. Gluck[2], N. Hubin[34], E. Hugot[6], M. Jaquet[6], M. Kasper[34,2], F. Madec[6], Y. Magnard[2], P. Martinez[25], D. Maurel[2], D. Le Mignant[6], O. Möller-Nilsson[13], M. Llored[6], T. Moulin[2], A. Origné[6], A. Pavlov[13], D. Perret[8], C. Petit[33], J. Pragt[35], P. Puget[2], P. Rabou[2], J. Ramos[13], F. Rigal[23], S. Rochat[2], R. Roelfsema[35], G. Rousset[8], A. Roux[2], B. Salasnich[1], J.-F. Sauvage[33], A. Sevin[8], C. Soenke[33], E. Stadler[2], M. Suarez[33], L. Weber[14], and F. Wildi[14]

(Affiliations can be found after the references)

Received 1 July 2020 / Accepted 3 February 2021

ABSTRACT

Context. Large surveys with new-generation high-contrast imaging instruments are needed to derive the frequency and properties of exoplanet populations with separations from ~5 to 300 au. A careful assessment of the stellar properties is crucial for a proper understanding of when, where, and how frequently planets form, and how they evolve. The sensitivity of detection limits to stellar age makes this a key parameter for direct imaging surveys.

Aims. We describe the SpHere INfrared survey for Exoplanets (SHINE), the largest direct imaging planet-search campaign initiated at the VLT in 2015 in the context of the SPHERE Guaranteed Time Observations of the SPHERE consortium. In this first paper we present the selection and the properties of the complete sample of stars surveyed with SHINE, focusing on the targets observed during the first phase of the survey (from February 2015 to February 2017). This early sample composed of 150 stars is used to perform a preliminary statistical analysis of the SHINE data, deferred to two companion papers presenting the survey performance, main discoveries, and the preliminary statistical constraints set by SHINE.

Methods. Based on a large database collecting the stellar properties of all young nearby stars in the solar vicinity (including kinematics, membership to moving groups, isochrones, lithium abundance, rotation, and activity), we selected the original sample of 800 stars that were ranked in order of priority according to their sensitivity for planet detection in direct imaging with SPHERE. The properties of the stars that are part of the early statistical sample were revisited, including for instance measurements from the *Gaia* Data Release 2. Rotation periods were derived for the vast majority of the late-type objects exploiting TESS light curves and dedicated photometric observations.

Results. The properties of individual targets and of the sample as a whole are presented.

Key words. stars: fundamental parameters – stars: rotation – stars: activity – stars: pre-main sequence – stars: kinematics and dynamics – planets and satellites: general

1. Introduction

Today's success in direct imaging of exoplanets is intimately connected to the pioneering work in the previous decades to develop adaptive optics (AO) systems, infrared detectors, coronagraphs, and differential imaging techniques for ground-based telescopes (Mawet et al. 2012; Chauvin 2018). With the advent of dedicated instruments on 5–10 m telescopes (e.g., LBT, Palomar, Subaru, Keck, VLT, Gemini, and *Magellan*), high-contrast imaging (HCI) demonstrated the ability to detect and characterize exoplanets and planetary systems, confirming that ground-based instrumentation may reach performance levels that could compete with those from space. Early large systematic surveys of young nearby stars led to the discovery of the first planetary-mass companions at large separations (>100 au) or with a low mass ratio relative to their stellar host (Chauvin et al. 2004, 2005b; Neuhäuser et al. 2005; Luhman et al. 2006; Lafrenière et al. 2008), followed by the breakthrough discoveries of closer

* Tables 5–11 are only available at the CDS via anonymous ftp to cdsarc.u-strasbg.fr (130.79.128.5) or via http://cdsarc.u-strasbg.fr/viz-bin/cat/J/A+A/651/A70

planetary-mass companions such as HR 8799 bcde (Marois et al. 2008, 2010), β Pictoris b Lagrange et al. (2009), κ And b (Carson et al. 2013), HD 95086 b (Rameau et al. 2013a), and GJ 504 b (Kuzuhara et al. 2013). This allowed a first systematic characterization of the giant planet population with separations typically ≥20–30 au (e.g., Biller et al. 2007; Lafrenière et al. 2007; Heinze et al. 2010; Chauvin et al. 2010, 2015; Vigan et al. 2012, 2017; Rameau et al. 2013b; Nielsen et al. 2013; Wahhaj et al. 2013; Brandt et al. 2014; Galicher et al. 2016; Bowler 2016). These early results confirmed that direct imaging is an important complementary technique in terms of discovery space with respect to other planet hunting techniques like radial velocity, transit, μ-lensing and astrometry (e.g., Johnson et al. 2010; Howard et al. 2010; Mayor et al. 2011; Sumi et al. 2011; Cassan et al. 2012; Bonfils et al. 2013; Meyer et al. 2018; Fernandes et al. 2019). Nowadays, direct imaging brings a unique opportunity to explore the outer part of exoplanetary systems with separations beyond ∼5 au to complete our view of planetary architectures, and to explore the properties of relatively cool giant planets. The advent of the new generation of extreme-AO planet imagers like SPHERE (Beuzit et al. 2019) and GPI (Macintosh et al. 2014) connected to systematic surveys of hundreds young nearby stars led to new discoveries like 51 Eri b (Macintosh et al. 2015), HIP 65426 b (Chauvin et al. 2017b), and PDS 70 b and c (Keppler et al. 2018; Haffert et al. 2019; Mesa et al. 2019). However, the low rate of discoveries despite the unprecedented gain in detection performance achieved with SPHERE and GPI showed that massive giant planets with an orbital semi-major axis beyond 10 au are rare (Nielsen et al. 2019).

On the other hand, the gain in performance allows a much better characterization of exoplanetary systems and exoplanets themselves. In direct imaging the exoplanet's photons can indeed be spatially resolved and dispersed to directly probe the atmospheric properties of exoplanets and brown dwarf companions. In comparison to generally older free-floating substellar objects, exoplanets discovered by high-contrast imaging are younger, hotter, and brighter. Their atmospheres show low-gravity features, and the presence of clouds and non-equilibrium chemistry processes. These physical conditions are very different and complementary to those observed in the atmospheres of hot Jupiters (observed in transmission or via secondary-eclipse). A large number of young brown dwarf and exoplanet atmospheres have been systematically characterized to test our current understanding of the processes at play in the atmospheres of substellar objects and to test evolutionary models including HR 8799 bcde (Ingraham et al. 2014; Bonnefoy et al. 2016; Greenbaum et al. 2018), 51 Eri b (Rajan et al. 2017; Samland et al. 2017), β Pictoris b (Chilcote et al. 2017), HD 95086 b (De Rosa et al. 2016; Chauvin et al. 2018), HIP 65426 b (Chauvin et al. 2017b; Cheetham et al. 2019), HIP 64892 B (Cheetham et al. 2018), and PDS 70 b and c (Müller et al. 2018; Mesa et al. 2019).

Regarding planetary architectures, relative astrometry at 1–2 mas precision with SPHERE and GPI opens up a new parameter space to carry out a precise monitoring of the orbital motion of a handful of exoplanets and brown dwarfs. This constrains their orbital properties and allows the exploration of the dynamical stability of the whole architecture. Examples of systems for which this analysis was done include β Pictoris (Wang et al. 2016; Lagrange et al. 2019), HR 8799 (Wang et al. 2018), HD 95086 (Rameau et al. 2016; Chauvin et al. 2018), HR 2562 (Maire et al. 2018), 51 Eri (Maire et al. 2019; De Rosa et al. 2020), and GJ 504 (Bonnefoy et al. 2018).

The current instrumentation does not yet allow us to detect mature planets reflecting star light, except perhaps for the closest and brightest stars. The focus of direct imaging programs is therefore on thermal emission from young planets because they are expected to be brighter than their older counterparts. For this same reason they are very useful to directly probe the presence of planets within the environment where they form, the circumstellar disks. This allows us to connect the spatially resolved structures of circumstellar disks (e.g., warp, cavity, rings, vortices) with imaged or unseen exoplanets. This is a fundamental and inevitable path to understand the formation of giant planets, and more generally planetary architectures favorable to the formation of smaller rocky planets with suitable conditions to host life (Barbato et al. 2018; Bryan et al. 2019). Studying the demographics of exoplanets is particularly important in order to understand the architecture and the formation and evolution of exoplanets. Giant planets dominate the architecture of planetary systems from a dynamical point of view, with impact on the subsequent formation and evolution of smaller planets, the distribution of water in the system, and thus the chances for habitability.

Within this framework, we planned the SpHere INfrared survey for Exoplanets (SHINE; Chauvin et al. 2017a). This survey uses a total of 200 nights that were allocated in visitor mode (typically affected by 20% of poor conditions for AO) and makes up a large fraction of the SPHERE consortium Guaranteed Time Observations allocated by ESO for the design and construction of the SPHERE instrument (Beuzit et al. 2019). SHINE has been designed by the SPHERE consortium to: (i) identify new planetary and brown dwarf companions and provide a first-order characterization; (ii) study the architecture of planetary systems (multiplicity and dynamical interactions); (iii) investigate the link between the presence of planets and disks (in synergy with the GTO program aimed at disk characterization); (iv) determine the frequency of giant planets with semi-major axes beyond 5 au; and (v) investigate the impact of stellar mass (and even age if possible) on the frequency and characteristics of planetary companions over the range ∼0.5–3.0 $M_{\odot}$.

SHINE started in February 2015 and is planned to be completed by July 2021, with observation of a total of about 500 young nearby stars. This is the first in a series of three papers describing early results obtained from the analysis of about one-third of this very large sample, in which we consider only those targets whose first observation was done before February 2017. We chose this cut-off date as second-epoch observations with time separations of 1–2 yr were required for a large number of candidates to vet physical companions from field stars (mainly background). This sample, hereafter referred to as F150 (as it consists of 150 stars), is already large enough for a first statistical discussion of the incidence of massive planets at a separation ≥5 au, and to have a first indication of the formation scenarios for giant planets. This paper describes the general characteristics of the survey and the observed sample. A second paper (Langlois et al. 2021, Paper II) describes the observations and analysis methods, and presents the results in terms of detection and upper limits, while a third paper (Vigan et al. 2021, Paper III) presents the statistical analysis and a discussion of the implications, as derived from the F150 sample.

The paper is organized as follows: Sect. 2 describes the SHINE survey, its science goals, and the target selection criteria. Section 3 presents the selection of the complete SHINE sample and the priority ranking. Section 4 describes the F150 subsample used for the early statistical analysis. In Sect. 5, we derive the most relevant parameters of individual targets and in Sect. 6 we

present the ensemble properties of the sample. Section 7 summarizes the results. Appendix A includes notes on individual targets.

2. Design of the SHINE survey

In order to achieve its scientific goals, the design and selection of the SHINE sample was of prime importance to optimally exploit a total of 200 nights of Guaranteed Time Observations with SPHERE at VLT dedicated to this campaign. Since massive planets at large separations are rare with a typical frequency of a few percent (see, e.g. Vigan et al. 2017; Nielsen et al. 2019), several hundred targets must be surveyed in order to lead to new discoveries and set precise constraints on the occurrence of giant planets beyond 5 au. Having a sample that is complete (in terms of distance, age, or limiting magnitude) likely implies a low efficiency. On the other hand, a proper statistical discussion requires well-defined selection criteria. The approach we considered to combine these apparently conflicting issues was to start from a very large sample of potential targets for which a wide set of properties, including magnitude, distance, mass, and age, was known (determined by us). We then divided them into priority groups according to a figure of merit (FoM) determined from these properties. A higher value for this FoM implies a higher probability that a star has a planet possibly detectable by SPHERE according to a specified model describing the planet distribution. To reduce the possibility that results will be poor because the selected model is not appropriate, the final priority list was actually obtained combining rankings given by two completely different models (see Sect. 2.3). This approach allows a reasonably high efficiency in detecting planets combined with the requirement of well-defined selection criteria, that can be finally considered in the statistical analysis.

The survey design included the optimization of the number of visits versus observing time per visit. We adopted as a compromise a visit of about 1.5 h including pointing and AO setup overheads. This ensures a field rotation of ≥30 degrees for most declinations in the case of observations including the meridian passage, allowing good removal of the speckle patterns using angular differential imaging (ADI; Marois et al. 2006). Longer exposures provide little improvement because of the limited additional field rotation. Shorter exposures would allow us to observe more targets, but would imply significant degradation of the achievable contrast for individual observations. Considering that the available number of high-merit targets (nearby very young stars) is not particularly large (see below), this would imply a smaller number of expected detections.

In the original survey design we planned to devote 70% of the time to first-epoch observations, 20% to second epochs for common proper motion confirmation, and 10% to additional characterization observations, exploiting the variety of observing modes available for SPHERE. The estimate of the amount of time needed for second-epoch observations was based on predictions of the background star contamination rate in the SPHERE field of view using Galactic population models (e.g., Robin & Creze 1986) and our target coordinates.

The selected setup for the survey used the IRDIFS mode, allowing simultaneous observations in YJ range (0.95–1.35 μm using IFS (Claudi et al. 2008) over a small field of view ($1.77'' \times 1.77''$) and observations in two narrowband filters in H-band using IRDIS (Dohlen et al. 2008) over a $11'' \times 11''$ field of view. The two narrowband filters (H2 and H3, Vigan et al. 2010) were selected for their sensitivity to methane-dominated objects (H2–H3 ≤ 0.0 mag) and to very red, late L objects (H2–H3 ∼ 0.0–0.5 mag). Field stars have an H2–H3 color close to zero, allowing the implementation of a robust priority scheme for the confirmation of the candidates (see Paper II for details).

2.1. The SHINE database

Over the past 10 yr we assembled a large sample of young stars with the main goal of preparing the SHINE survey. This work included the determination of several stellar properties, either from the analysis of new observations or from the literature. The database was also used to select samples for other programs, such as the NaCo Large Program for Exoplanet Imaging (NaCo-LP; Chauvin et al. 2015), the SPOTS survey for circumbinary planets (Asensio-Torres et al. 2018), the HARPS Large Program for planets around young stars (Grandjean et al. 2020), the search for planets around young stars in the framework of the GAPS program at TNG (Carleo et al. 2020), and several other programs.

The determination of target parameters is mostly based on the methods described in the NaCo-LP target characterization paper (Desidera et al. 2015). Briefly, stellar ages were obtained from a combination of age methods (membership to groups, lithium, rotation, activity, kinematics, isochrone fitting). Moving groups (MGs) membership was taken from Torres et al. (2008), with updates from the literature in the following years. Ages of moving groups were those adopted by Desidera et al. (2015) (their Table 8). Stellar distances were taken from HIPPARCOS trigonometric parallax when available (van Leeuwen 2007), otherwise the (age-dependent) photometric distances derived as done in Desidera et al. (2015) were adopted. Stellar masses were derived following the Reid et al. (2002) calibrations. The original values of stellar mass, distance, and age are listed in Table 11. Comparison with the updated values derived in this paper (Sect. 5) shows a nice agreement for the distance (mean difference 3.7 pc, rms 9.4 pc), a small offset in stellar age (0.13 dex with rms 0.21 dex, with the original ages being younger), and a systematic difference in stellar masses above 1.8–2.0 $M_{\odot}$ (the original mass being smaller) and a fairly good agreement below this value. This last difference has some impact on the actual upper limit in mass for the sample (see below), but otherwise the use of the original parameters with respect to the updated ones derived in this paper should have a minor impact on the target selection and the priority scheme defined below. Originally the sample was limited to distances closer than 100 pc; it was complemented with stars in the Sco-Cen OB association (e.g., de Zeeuw et al. 1999) to reach a suitable number of young, early-type stars (from early F to late B) at slightly larger distances.

For the final selection of the SHINE sample, we first identified some general selection criteria, driven by the characteristics of the SPHERE instrument (coordinates of the site; magnitude limit for good performance of the AO system) or by the science goals described above. The following selection criteria were set:

1. Declination limits between −84 and +21 degrees to ensure observations at airmass values of less than 2;
2. Wavefront sensor (WFS) flux[1] >5 e-/subpup/frame or $R \leq 11.5$ (to ensure good quality of AO correction, being on the conservative side of estimates from the SPHERE performance simulations available at the time of target selection);
3. Exclusion of known spectroscopic and close visual binaries (projected separation <6 arcsec, i.e., within the IRDIS

[1] Flux as seen by the SPHERE WFS sensor; see Beuzit et al. (2019) for details.

field of view)[2]. This is motivated by the technical limitations of AO working and ADI processing for spatially resolved binaries and by our scientific choice of having a homogeneous sample of single stars or components of wide binaries without the complications of the severe dynamical influence of stellar companions or of uncertain process of planet formation and evolution in circumbinary disks;
4. Age <800 Myr because planets are too faint at older ages for wavelengths <2.3 μm;
5. Distance <100 pc to probe the smallest physical separations, except for Sco-Cen members, as this region is rich in young early-type stars;
6. $M_* < 3\ M_\odot$. This limit was set because the frequency of planets detected using radial velocities (RV) appears to drop above this mass (Reffert et al. 2013). We did not set any explicit lower-mass cutoff, though an implicit limit was set by the requirement on AO flux. Our survey then covers the full range 0.5–3.0 $M_\odot$, which allows us to explore the influence of stellar mass.

The sample has no explicit biases related to the presence of disks nor to metallicity. At young ages metallicity determinations are quite sparse (Biazzo et al. 2012; Viana Almeida et al. 2009). The available results point toward a metallicity close to solar for stars younger than ~200 Myr in the solar vicinity. The metallicity dispersion becomes significant for older stars, which constitute a very small fraction of our sample.

The resulting list satisfying the above criteria at the time of freezing the SHINE sample (May–August 2014) included 1224 targets; this is larger by about 50% with respect to the sample to be selected (800 stars), which in turn is almost twice the number of stars that could be effectively observed.

2.2. Target priorities

A well-defined priority scheme is necessary in order to run an efficient survey on a sample of several hundred targets because the potential for exoplanet discovery is very different from star to star, depending on age, distance, mass, and magnitude. Ideal targets are very young stars close to the Sun. Simulations described in Sect. 2.3 were performed on this extended list in order to estimate the potential for planet detectability of each target and drive the final target selection.

The priority assignment applied to the SHINE database is the following:

1. Build a FoM that allows the stars to be ranked according to the probability that they host planets potentially detectable by SPHERE. To estimate this probability, we used (i) planet population models based on power laws in planet mass and separation, with cutoffs at large separations; combined with stellar ages this enables the planet luminosity to be estimated via suitable evolution models; (ii) the MESS code (Multipurpose Exoplanet Simulation System, see Bonavita et al. 2012, 2013, for details)[3] that allows the planet position to be projected on the sky at the epoch of observation; and (iii) expected contrast limits appropriate for each star given the stellar properties (distance, age, magnitude). These three different aspects of the construction of the FoM are described in the next subsection.
2. Sort the parent sample according to this FoM and construct an optimal 400 star sample as high priority (List 400), and complete it with additional targets to fill in according to rank order, lower priority, up to 100% over-subscription (List 400+). The final sample reaches 800 stars[4].
3. Check that this optimized-for-detections sample covers a reasonably wide distribution in stellar mass.
4. Consider some adaptions of this sample, such as (i) inclusion of homogeneous subsamples, as volume-limited members of nearby young moving groups and (ii) limiting the number of Sco-Cen members to 20% of the sample because these stars have a limited span in right ascension, and the background contamination is often large due to their low galactic latitude, which has a severe impact on the expected need for second-epoch observations.

2.3. Simulations of planet detectability

In order to define the FoM to be used to select the final SHINE sample, we estimated the expected survey yield as a function of the target list as well as the assumptions on the underlying characteristics of the planet population. For this purpose we used the MESS (see Bonavita et al. 2012, for details) code to evaluate the probability of detecting a companion given the expected instrument performance. The synthetic companions were generated according to two different models, both based on the one described by Cumming et al. (2008), that is, adopting power-law distributions for the companion mass and semi-major axis.

Both models are defined so that the resulting frequency of companions F is consistent with the value of the fraction of planets per star retrieved by Cumming et al. (2008) ($F_0 = 0.0394$) if calculated over the same parameter space (mass: 1–13 $M_{\rm Jup}$, semi-major axis: 0.3–2.5 au, stellar mass: 0.7–1.6 $M_\odot$, [Fe/H]: −0.5–+0.5). This implies the use of a normalization factor C_0 defined as follows:

$$F_0 = C_0 \int_{0.7\ M_\odot}^{1.6\ M_\odot} \mathrm{d}M * \int_{1\ M_{\rm Jup}}^{13\ M_{\rm Jup}} m^{-1.3}\ \mathrm{d}m \int_{0.3\ \mathrm{au}}^{2.5\ \mathrm{au}} a^{-0.61}\ \mathrm{d}a \qquad (1)$$

The companion mass range was fixed at $m_{\rm max} = 75\ M_{jup}$ for all the targets in the first model (hereafter Mod01). For the second model (hereafter Mod02) we instead adopted $m_{\rm max} = 0.03 \times M_* \frac{M_{\rm Jup}}{M_\odot}$. Mod02 also includes a dependency on the stellar mass for the expected value of the frequency. For this model the normalization factor is in fact expressed as $C_0 f(M_*)$, where $f(M_*)$ is a mass function that ensures that the resulting number of companions increases linearly with stellar masses up to 2 $M_\odot$, and is zero for stellar masses higher than 3 $M_\odot$, following the findings of Reffert et al. (2013) for close-in planets.

The main difference between the two models is therefore that for Mod02 the properties of the generated planet population are not fixed, but change for each target. For this reason, a ranking based only on Mod02 would introduce a bias towards A–F stars. The use of both models combined instead supports the selection of a more balanced sample, which is necessary to assess the dependence of planet frequency on stellar mass, which is one of the main scientific drivers of the survey.

For all the stars in the initial list we evaluated the expected SPHERE detection limits, expressed in terms of luminosity contrast versus projected separation (shown in the left panel of

[2] Preparatory observations of part of the sample were performed with FEROS (Mouillet et al. 2010; Desidera et al. 2015) and with AstraLux (Hormuth et al. 2008).

[3] An updated version of the MESS code, now called Exoplanet Detection Map Calculator (Exo-DMC Bonavita 2020), is available for download at https://github.com/mbonav/Exo_DMC

[4] This is significantly larger than the sample size allowed by the available observing time, but we decided to oversize the sample in order to have enough flexibility on the scheduling, considering the requirement of observing the targets including the meridian passage.

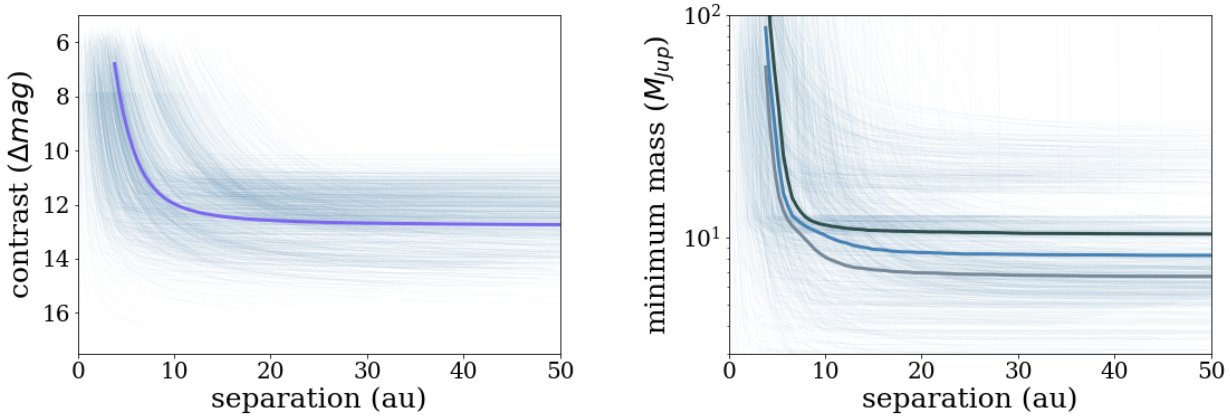

Fig. 1. Expected IFS detection limits (light blue curves), evaluated using the method described in Mesa et al. (2015), expressed in terms of contrast (*left panel*) or minimum companion mass (*right panel*, calculated assuming the best age for each target). The solid blue line shows the average over the full input sample. The light and dark gray curves in the right panel show the average mass limit obtained adopting the minimum and maximum values of the age, respectively.

Fig. 1), using the method described in Mesa et al. (2015). The models of Baraffe et al. (2003) were then used to estimate the corresponding minimum detectable companion mass $M_{\rm lim}$[5] (see Fig. 1, right panel), under the assumption that any companion would be coeval with its host star, hence using the age of the star to select the appropriate evolutionary track. To take into account the fact that the detection limits are expressed in projected separation, while the models produces semi-major axis values, the code evaluates the probability that a companion with a given semi-major axis can have a projected separation which would put it inside the field of view (FoV). This is done assuming a random orbital phase and eccentricity drawn from a Gaussian distribution (see Bonavita et al. 2012, for details).

For each model we performed six MESS runs, using the list of 1244 targets from the SHINE database, but changing the following parameters:

– the value of the age used for the magnitude to mass conversion of the detection limits (the adopted age of each star, as well as the minimum and maximum values) in order to properly estimate the impact of the uncertainty on the age on the survey results.
– the cutoff of the semi-major axis distribution, which was set at 15 or 30 au (a value of 50 au was used for the Sco-Cen members to take into account the larger distance of this region with respect to the other targets in the list)[6].

Table 1 summarizes the outcome of the simulations, in terms of expected detection yield, assuming a sample made of the best 400 targets ranked according to each model. The values obtained using the 15 au and the 30 au cutoff values are both shown, and those obtained using the minimum and maximum values of the stellar age for the magnitude to mass conversion of all the detection limits.

Table 1. Summary of the expected detection yield for the best 400 targets ranked according to the different models.

Model, cutoff	Number of expected detections			Sco-Cen
	Adopt. age	Min. age	Max. age	Members
Mod01, 15 au	24.73	28.29	22.41	15
Mod01, 30 au	48.27	53.65	44.82	35
Mod02, 15 au	16.12	18.89	14.25	2
Mod02, 30 au	30.22	34.25	27.12	12

Notes. The same values obtained considering the minimum and maximum estimated age of each target are also shown. The number of Sco-Cen members (for which the cutoff is always 50 au) is reported in the last column.

The expected number of detections in Table 1 is larger than the actual number (although the final number of detection from SHINE is not yet available, pending the completion of the second-epoch observations). This indicates that some of the assumptions we made in the simulations are not adequate. The dependency of planet frequency on semi-major axis is likely the most prominent case. There were already hints at the time of the sample selection that the extrapolations of RV-based power laws with outer cutoff are not ideal, considering both the few individual detections at very wide separations, and low frequency of substellar companions resulting from various surveys. However, alternative distributions such the log-normal distribution by Meyer et al. (2018) were published a few years later. Therefore, we were expecting the outcome of our simulations to be overestimating the number of new discoveries since the beginning of the survey, and in this perspective we planned only a limited amount of time for characterization observations in the original survey design (see Sect. 2). In spite of these limitations, we consider our simulations appropriate for the main aim of the priority ranking, which is to build a good sample to answer our scientific questions (e.g., including a broad range of stellar masses).

[5] Alternative sets of models available at the time of sample building were considered but not used because of the lack of grid covering our space of parameters of our interest and/or because of counter-examples already available at that time against some of these models, such as the extreme cold-start scenario by Marley et al. (2007).

[6] This allowed us a proper ranking of the Sco-Cen targets, which would not be reliable for closer cutoff values. A cutoff as large as 50 au was already ruled out at the time of the sample selection for solar-type stars. The situation was less clear for more massive stars, with possible scaling of planet distribution in mass (following the mass ratio) and in separation (following the loction of the snow line). Considering the roughly flat sensitivity curve of SPHERE at separation larger than 0.3″, this simulation was roughly equivalent from the point of view of the ranking the Sco-Cen targets to a more realistic one with a low-frequency but broad distribution at wide separation. This inhomogeneity has no consequences in the final sample selection, considering that we included a fixed number of Sco-Cen targets for each priority bin (see Sect. 3).